Nonlinear stability results for plane Couette and Poiseuille flows

Paolo Falsaperla, Andrea Giacobbe,* and Giuseppe Mulone
Università degli Studi di Catania, Dipartimento di Matematica e Informatica, Viale A. Doria 6, 95125 Catania, Italy

(Received 8 February 2019; revised manuscript received 26 April 2019; published 26 July 2019)

We prove that the plane Couette and Poiseuille flows are nonlinearly stable if the Reynolds number is less than $\mathrm{Re}_{\mathrm{Orr}}(2\pi/(\lambda\sin\theta))/\sin\theta$ when a perturbation is a tilted perturbation in the direction x' which forms an angle $\theta \in (0, \pi/2]$ with the direction $\mathbf{i}$ of the basic motion and does not depend on x'. $\mathrm{Re}_{\mathrm{Orr}}$ is the critical Orr-Reynolds number for spanwise perturbations which is computed for wave number $2\pi/(\lambda\sin\theta)$, with λ being any positive wavelength. By taking the minimum with respect to λ, we obtain the critical energy Reynolds number for a fixed inclination angle and any wavelength: for plane Couette flow, it is $\mathrm{Re}_{\mathrm{Orr}} = 44.3/\sin\theta$, and for plane Poiseuille flow, it is $\mathrm{Re}_{\mathrm{Orr}} = 87.6/\sin\theta$ (in particular, for $\theta = \pi/2$ we have the classical values $\mathrm{Re}_{\mathrm{Orr}} = 44.3$ for plane Couette flow and $\mathrm{Re}_{\mathrm{Orr}} = 87.6$ for plane Poiseuille flow). Here the nondimensional interval between the planes bounding the channel is $[-1, 1]$. In particular, these results improve those obtained by Joseph, who found for streamwise perturbations a critical nonlinear value of 20.65 in the plane Couette case, and those obtained by Joseph and Carmi who found the value 49.55 for plane Poiseuille flow for streamwise perturbations. If we fix some wavelengths from the experimental data and the numerical simulations, the critical Reynolds numbers that we obtain are in a very good agreement both with the the experiments and the numerical simulation. These results partially solve the Couette-Sommerfeld paradox.

DOI: 10.1103/PhysRevE.100.013113

I. INTRODUCTION

The study of stability and instability of the classical laminar flows of an incompressible fluid has attracted the attention of many authors for more than 150 years: Stokes, Taylor, Couette [1], Poiseuille [2], Kelvin [3], Reynolds [4], Lorentz, Orr [5], Sommerfeld [6], Squire [7], Joseph [8], Busse [9], and many others.

This problem is nowadays the object of study (see, for instance, Deng and Masmoudi [10], Bedrossian *et al.* [11], Lan and Li [12], Cherubini and De Palma [13], Liefvendahl and Kreiss [14]) because the transition from laminar flows to instability, turbulence, and chaos is not completely understood and there are some discrepancies between the linear and nonlinear analysis and the experiments (the so-called Couette-Sommerfeld paradox).

We observe that many different conventions are used in the literature to nondimensionalize the width of the channel. Here we follow Prigent *et al.* [15] who generalize the Reynolds number used in plane Couette flow $U = z/d$ by considering it as based on the (average) shear and the half gap d: $\mathrm{Re} = Ud/\nu$ [see also Barkley and Tuckerman [16], Eq. (A1)].

For Poiseuille flow, we use the Reynolds number based on velocity units of the undisturbed stream velocity at the center of the channel and the half gap d. Only at the end of the paper, in order to compare with the results of Tsukahara *et al.* [17], do we define a Reynolds number based on the average shear and half gap [see Barkley and Tuckerman [16], Eqs. (A10)–(A12)].

The classical results are the following:

(a) Plane Poiseuille flow is *unstable* for $\mathrm{Re} > 5772$ (see Orszag [18]).

(b) Plane Couette flow and pipe Poiseuille flow (in the axisymmetric case) are *linearly stable for all* Reynolds numbers (see Romanov [19] and Zikanov [20]).

(c) In laboratory experiments, plane and pipe Poiseuille flows undergo a transition to three-dimensional turbulence for Reynolds numbers of the order of 1000. In the case of plane Couette flow, the lowest Reynolds numbers at which turbulence can be produced and sustained have been shown to be between 300 and 450, both in the numerical simulations and in the experiments.

(d) Nonlinear asymptotic *L_2-energy stability* has been proven for Reynolds numbers Re below some critical nonlinear value Re_E which is of the order of 10^2. In particular, Joseph [21] proved that $\mathrm{Re}_E = \mathrm{Re}_E{}^y = 20.65$ (and $\mathrm{Re}_E{}^x = 44.3$) for plane Couette flow, and Joseph and Carmi [22] proved that $\mathrm{Re}_E = \mathrm{Re}_E{}^y = 49.55$ (and $\mathrm{Re}_E{}^x = 87.6$) for plane Poiseuille flow. Here and in what follows, Re^y refers to the critical value for streamwise (or longitudinal) perturbations and Re^x refers to the critical value for spanwise (or transverse) perturbations.

The use of *weighted L_2 energy* has been fruitful for studying nonlinear stability in fluid mechanics (see Straughan [23]). Rionero and Mulone [24] studied the nonlinear stability of parallel shear flows with the Lyapunov method in the (ideal) case of stress-free boundary conditions. By using a weighted energy, they proved that plane Couette flows and plane Poiseuille flows are conditionally asymptotically stable for all Reynolds numbers.

Kaiser *et al.* [25] wrote the velocity field in terms of poloidal, toroidal, and mean-field components. They used a generalized energy functional $\mathcal{E}$ (with some coupling parameters chosen in an optimal way) for *plane Couette* flow, providing conditional nonlinear stability for Reynolds numbers Re

*Corresponding author: giacobbe@dmi.unict.it

below $\mathrm{Re}_{\mathcal{E}} = 44.3$, which is larger than the ordinary energy-stability limit. The method allows the explicit calculation of so-called stability balls in the $\mathcal{E}$ norm, i.e., the system is stable with respect to any perturbation with $\mathcal{E}$ norm in this ball.

Kaiser and Mulone [26] proved conditional nonlinear stability for *arbitrary plane parallel shear flows* up to some value Re_E which depends on the shear profile. They used a generalized (weighted) functional E and proved that Re_E turns out to be Re_E^x, the ordinary energy-stability limit for perturbations independent of y (spanwise perturbations). In the case of the experimentally important profiles, viz., linear combinations of Couette and Poiseuille flow, this number is at least 87.6, the value for pure Poiseuille flow. For Couette flow, it is at least 44.3.

Li and Lin [27] and Lan and Li [12] gave a contribution towards the solution of the Sommerfeld paradox. They argue that even though the linear shear is linearly stable, slow orbits (also called quasisteady states) in arbitrarily small neighborhoods of the linear shear can be linearly unstable. They observe: "The key is that in infinite dimensions, smallness in one norm does not mean smallness in all norms" [12], p. 1. Their study focuses upon a sequence of two-dimensional (2D) oscillatory shears which are the Couette linear shear plus small-amplitude and high spatial frequency sinusoidal shear perturbations.

Butler and Farrell [28] observed that transition to turbulence in plane channel flow occurs even for conditions under which modes of the linearized dynamical system associated with the flow are stable. By using variational methods, they found linear three-dimensional perturbations that gain the most energy in a given time period.

Cherubini and De Palma [13] used a variational procedure to identify nonlinear optimal disturbances in a Couette flow, defined as those initial perturbations yielding the largest energy growth at a short target time T, for given Reynolds number Re and initial energy E_0.

Recently, Bedrossian *et al.* [11] studied Sobolev regularity disturbances to the periodic, plane Couette flow in 3D incompressible Navier-Stokes equations at high Reynolds number Re with the goal to estimate the stability threshold—the size of the largest ball around zero in a suitable Sobolev space H^σ—such that all solutions remain close to Couette. In particular, they proved the following remarkable result: "Initial data that satisfies $\|u_{in}\|_{H^\sigma} < \delta \mathrm{Re}^{-3/2}$ for any $\sigma > 9/2$ and $\delta = \delta(\sigma) > 0$ depending only on σ is global in time, remains within $O(\mathrm{Re}^{-1/2})$ of the Couette flow in L^2 for all time, and converges to the class of '2.5-dimensional' streamwise-independent solutions referred to as *streaks* for times $t \gtrsim \mathrm{Re}^{1/3}$" [11], p. 541.

Prigent *et al.* [15] conducted experiments at the CEA-Sanclay Centre to study, by decreasing the Reynolds number, the reverse transition from the turbulent to the laminar flow. At the beginning of their paper, they wrote: "In spite of more than a century of theoretical and experimental efforts, the transition to turbulence in some basic hydrodynamical flows is still far from being fully understood. This is especially true when linear and weakly nonlinear analysis cannot be used" [15, p. 100]. They further observed that "a continuous transition towards a regular pattern made of periodically spaced, inclined stripes of well-defined width and alternating turbulence strength...." [15, p. 100] "For lower Re, a regular pattern is eventually reached after a transient during which domains, separated by wandering fronts, compete. The oblique stripes have a wavelength of the order of 50 times the gap. The pattern is stationary in the plane Couette flow case …The pattern was observed for $340 < \mathrm{Re} < 415$ in the plane Couette flow", [15, p. 102].

Barkley and Tuckerman [16,29,30] studied numerically a turbulent-laminar banded pattern in plane Couette flow which is statistically steady and is oriented obliquely to the streamwise direction with a very large wavelength relative to the gap. They wrote: "Regimes computed for a full range of angle and Reynolds number in a tilted rectangular periodic computational domain are presented...The unusual but key feature of our study of turbulent-laminar patterns is the use of simulation domains aligned with the pattern wave vector and thus tilted relative to the streamwise-spanwise directions of the flow" [16], p. 109, p. 111. For their numerical simulations, they are guided by the experiments of Prigent *et al.* [15]. In their numerical simulation, the domain is oriented such that "the streamwise direction is tilted at angle $\theta = 24^\circ$ to the x-direction" [16], p. 112. In their Table 3, they, in particular, reported turbulent-laminar banded patterns in plane Couette and plane Poiseuille flows. Parameters reported by Prigent *et al.* [15] and in other papers are converted to a uniform Reynolds number based on the average shear and half gap. They show, for plane Couette flow, two columns that correspond to the values at the minimum and maximum reported Reynolds number: $\mathrm{Re} = 340$ for $\theta = 37^\circ$ and $\mathrm{Re} = 395$ for $\theta = 25^\circ$. For plane Poiseuille flow, one has (values from Tsukahara *et al.* [17]) the following: $\mathrm{Re} = 357.5$ for $\theta = 24^\circ$ and wavelength $\lambda = 41$.

We recall that Moffat [31] proved the stability of the basic motion with respect to 2D-streamwise perturbations for any Reynolds number. Here we give sufficient energy linear and nonlinear stability conditions of the basic plane Couette and Poiseuille flows with respect to tilted perturbations (see the definition below), which form an angle θ with the stream direction (x direction), for any Reynolds number less than the critical number,

$$\bar{R} = \frac{\mathrm{Re}_{\mathrm{Orr}}(2\pi/(\lambda \sin\theta))}{\sin\theta},$$

where $\mathrm{Re}_{\mathrm{Orr}}$ is the Orr [5] critical Reynolds number for spanwise perturbations evaluated at the wave number $2\pi/(\lambda \sin\theta)$. These results, in particular, confirm the results of Orr and improve those obtained by Joseph [21] and Joseph and Carmi [22]. Moreover, we note that for fixed wavelengths, from experiments and numerical simulations, our results are in a good agreement with the experiments of Prigent *et al.* [15] and the numerical computations of Barkley and Tuckerman [16], and Tsukahara *et al.* [17].

We underline that the scope of the paper is to find sufficient energy-stability conditions under which the basic translational motion (plane Couette or Poiseuille flows) is stable against tilted perturbations and compare the obtained critical Reynolds numbers with those of the experiments. We do not investigate the type of the turbulence at the criticality as done in the experiments and in the numerical simulations. Moreover, our critical energy Reynolds numbers hold for tilted perturbations both in the linear and nonlinear case.

The plan of the paper is the following. In Sec. II, we write the nondimensional perturbation equations of laminar flows in a channel and we recall the classical linear stability and instability results. We study the linear stability with the classical L_2 energy and obtain the critical Reynolds numbers found by Orr [5]. In Sec. III, we give sufficient nonlinear stability conditions of the plane Couette and Poiseuille flows with respect to tilted perturbations of an angle θ with respect to the direction of the motion and prove that they are nonlinearly exponentially stable for any Reynolds number less than

$$\frac{\mathrm{Re}_{\mathrm{Orr}}(2\pi/(\lambda\sin\theta))}{\sin\theta},$$

where $\mathrm{Re}_{\mathrm{Orr}}$ is the critical Reynolds number for spanwise perturbations defined above. In Sec. IV, we make a comparison with the experimental and numerical results and give some final comments.

II. LAMINAR FLOWS BETWEEN TWO PARALLEL PLANES

Consider, in a reference frame $Oxyz$ with unit vectors $\mathbf{i}, \mathbf{j}, \mathbf{k}$, the layer $\mathcal{D} = \mathbb{R}^2 \times [-d, d]$ of thickness $2d$ with horizontal coordinates x, y and vertical coordinate z.

Laminar shear flows $\mathbf{U} = U(z)\mathbf{i}$, $p = p(x)$ are solutions to the stationary Navier-Stokes equations,

$$\begin{cases} -\mathbf{U}\cdot\nabla\mathbf{U} + \nu\Delta\mathbf{U} - \nabla\bar{p} = \mathbf{0}, \\ \nabla\cdot\mathbf{U} = 0, \end{cases} \tag{1}$$

where $\mathbf{U}$ is the velocity field, $\bar{p}$ is the pressure, ν is the kinematic viscosity, ∇ is the gradient operator, and Δ is the Laplacian.

To nondimensionalize the equations and the gap of the layer, in the *Couette case*, we use a Reynolds number based on the shear and half gap d. So we obtain the nondimensional domain $\mathcal{D}_C = \mathbb{R}^2 \times [-1, 1]$ of thickness 2 with horizontal nondimensional coordinates x, y and nondimensional vertical coordinate z.

Couette flow, i.e., the solution of the Navier-Stokes equations, is then characterized by the functional form

$$\mathbf{U} = f(z)\mathbf{i} = z\mathbf{i}. \tag{2}$$

The function $z : [-1, 1] \to \mathbb{R}$ is the shear profile.

In the case of *Poiseuille flow*, we have the nondimensional domain $\mathcal{D}_{1P} = \mathbb{R}^2 \times [-1, 1]$ and

$$\mathbf{U} = f(z)\mathbf{i} = (1 - z^2)\mathbf{i}. \tag{3}$$

The perturbation equations to the plane parallel shear flows, in nondimensional form, are

$$\begin{cases} u_t = -\mathbf{u}\cdot\nabla u + \mathrm{Re}^{-1}\Delta u - (fu_x + f'w) - \frac{\partial p}{\partial x}, \\ v_t = -\mathbf{u}\cdot\nabla v + \mathrm{Re}^{-1}\Delta v - fv_x - \frac{\partial p}{\partial y}, \\ w_t = -\mathbf{u}\cdot\nabla w + \mathrm{Re}^{-1}\Delta w - fw_x - \frac{\partial p}{\partial z}, \\ \nabla\cdot\mathbf{u} = 0, \end{cases} \tag{4}$$

where $\mathbf{u} = u\mathbf{i} + v\mathbf{j} + w\mathbf{k}$ is the perturbation to the velocity field, p is the perturbation to the pressure field, and Re is the Reynolds number.

Throughout the paper, we use the symbols h_x as $\frac{\partial h}{\partial x}$, h_t as $\frac{\partial h}{\partial t}$, etc., for any function h.

To system (4), we append the rigid boundary conditions

$$\mathbf{u}(x, y, \pm 1, t) = 0, \quad (x, y, t) \in \mathbb{R}^2 \times (0, +\infty),$$

and the initial condition

$$\mathbf{u}(x, y, z, 0) = \mathbf{u_0}(x, y, z) \quad \text{in } \mathcal{D}_C \text{ or } \mathcal{D}_P,$$

with $\mathbf{u_0}(x, y, z)$ the solenoidal vector which vanishes at the boundaries.

We recall that the *streamwise* (or longitudinal) perturbations are the perturbations $\mathbf{u}$, p which do not depend on x, i.e., they are translational invariant in the downstream direction; the *spanwise* (or transverse) perturbations are the perturbations $\mathbf{u}$, p which do not depend on y.

We note that for spanwise perturbations, either $v \to 0$ exponentially fast as $t \to \infty$ or $v \equiv 0$.

Linear stability and instability

Assume that both $\mathbf{u}$ and ∇p are x, y periodic with wavelengths l_1 and l_2 in the x and y directions, respectively, with wave numbers $(a_1 = 2\pi/l_1, b_1 = 2\pi/l_2) \in \mathbb{R}^2_+$. In the following, it suffices therefore to consider functions over the periodicity cell,

$$\Omega = [0, l_1] \times [0, l_2] \times [-1, 1].$$

We recall that the classical results of Romanov [19] prove that plane Couette flow is *linearly stable* for *any Reynolds* number. Instead, plane Poiseuille flow is unstable for any Reynolds number bigger than 5772 (see Orszag [18]).

We observe that in the linear case, the Squire theorem holds and the most destabilizing perturbations are two dimensional, in particular the spanwise perturbations (see Drazin and Reid [32], p. 155). The critical Reynolds value, for Poiseuille flow, can be obtained by solving the celebrated Orr-Sommerfeld equation (see Drazin and Reid [32]).

As the basic function space, we take $L_2(\Omega)$, which is the space of square-integrable functions in Ω with the scalar product denoted by

$$(g, h) = \int_0^{l_1}\int_0^{l_2}\int_{-1}^{1} f(x, y, z)g(x, y, z)dxdydz$$

and the norm given by

$$\|f\| = \left[\int_0^{l_1}\int_0^{l_2}\int_{-1}^{1} f^2(x, y, z)dxdydz\right]^{1/2}.$$

We note that if we study the linear stability with the Lyapunov method, by using the classical energy

$$V(t) = \tfrac{1}{2}[\|u\|^2 + \|v\|^2 + \|w\|^2],$$

we obtain *sufficient conditions of linear stability*.

The Orr-Reynolds energy identity is given by

$$\dot{V} = -(f'w, u) - \mathrm{Re}^{-1}[\|\nabla u\|^2 + \|\nabla v\|^2 + \|\nabla w\|^2], \tag{5}$$

where $\dot{V}$ is the *orbital time derivative* [i.e., the Lagrangian derivative computed along the solutions of (4)]. To obtain (5), it is sufficient to integrate in Ω and take into account the zero-boundary conditions at the planes $z = -1$ and $z = 1$, the

periodicity in x and y, and the solenoidality of the perturbation velocity field $\mathbf{u}$.

We have

$$\begin{aligned}\dot{V} &= -(f'w,u) - \mathrm{Re}^{-1}[\|\nabla u\|^2 + \|\nabla v\|^2 + \|\nabla w\|^2] \\ &= \left(\frac{-(f'w,u)}{\|\nabla u\|^2+\|\nabla v\|^2+\|\nabla w\|^2} - \frac{1}{\mathrm{Re}}\right)\|\nabla \mathbf{u}\|^2 \\ &\leqslant \left(\frac{1}{\bar{R}} - \frac{1}{\mathrm{Re}}\right)\|\nabla \mathbf{u}\|^2,\end{aligned} \tag{6}$$

where

$$\frac{1}{\bar{R}} = \max_{\mathcal{S}} \frac{-(f'w,u)}{\|\nabla u\|^2 + \|\nabla v\|^2 + \|\nabla w\|^2}, \tag{7}$$

and $\mathcal{S}$ is the space of the *kinematically admissible fields*,

$$\begin{aligned}\mathcal{S} = \{u, v, w \in H^1(\Omega),\ u = v = w = 0 \quad \text{on the boundaries},\\ u_x + v_y + w_z = 0, \quad \|\nabla u\| + \|\nabla v\| + \|\nabla w\| > 0\}.\end{aligned} \tag{8}$$

Here, $H^1(\Omega)$ is the Sobolev space of the functions which are in $L_2(\Omega)$ together with their first generalized derivatives.

The Euler-Lagrange equations of this maximum problem are given by

$$\bar{R}(f'w\mathbf{i} + f'u\mathbf{k}) - 2\Delta\mathbf{u} = \nabla\lambda, \tag{9}$$

where λ is a Lagrange multiplier.

Since, for spanwise perturbations, $v \equiv 0$ and $\frac{\partial}{\partial y} \equiv 0$, by taking the third component of the *double curl* of (9) and by using the solenoidality condition $u_x + w_z = 0$, we obtain the *Orr equation* [5]

$$\frac{\bar{R}}{2}(f''w_x + 2f'w_{xz}) + \Delta\Delta w = 0, \tag{10}$$

with no-slip boundary conditions $w = w_z = 0$ on $z = \pm 1$.

By solving this equation, with the given boundary conditions, we obtain the Orr results: for Couette and Poiseuille flows, we have $\mathrm{Re}_{\mathrm{Orr}} = \bar{R} = 44.3$ (cf. Orr [5], p. 128) and $\mathrm{Re}_{\mathrm{Orr}} = \bar{R} = 87.6$ (cf. Drazin and Reid [32], p. 163), respectively.

III. NONLINEAR STABILITY

Nonlinear stability conditions have been obtained by Orr in a celebrated paper, by using the Reynolds energy method (see Orr [5], p. 122). In fact, the energy method used for linear system in Sec. II still holds in the nonlinear case because, by taking into account of the boundary conditions and the periodicity, the integrated cubic nonlinear terms vanish.

Orr writes: "Analogy with other problems leads us to assume that disturbances in two dimensions will be less stable than those in three; this view is confirmed by the corresponding result in case viscosity is neglected" [5, p. 125]. He also says: "The three-dimensioned case was attempted, but it proved too difficult" [5, p. 125].

Orr considers spanwise perturbations (i.e., $v \equiv 0$ and $\frac{\partial}{\partial y} \equiv 0$), the same perturbations that are used in the linear case by using Squire transformation (cf. Squire [7]; Drazin and Reid [32]).

The critical value that he found, in the Couette case, is $\mathrm{Re}^x = 44.3$, where Re^x *is the critical Reynolds number with respect to spanwise perturbations* (see Orr [5], p. 128; Joseph [8], p. 181).

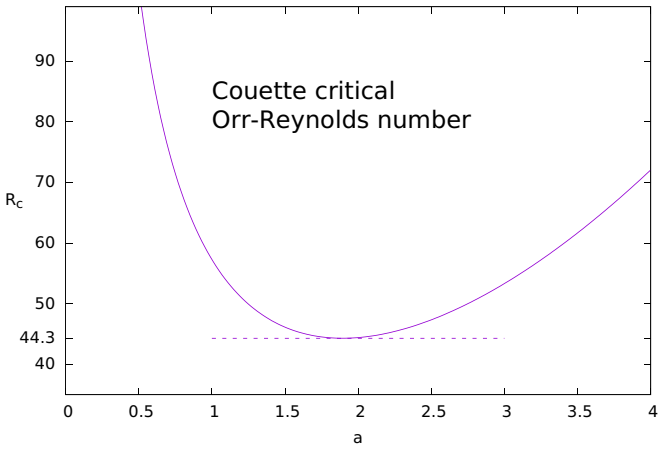

FIG. 1. Plane Couette energy Orr-Reynolds number $\bar{R} = R_c$ as a function of the wave number a, for Eq. (10) with nonslip boundary conditions. The absolute minimum is $R_c = 44.3$ and it is achieved when the wave number $a_c = 1.9$. Here the channel has gap 2 and $z \in [-1, 1]$.

Joseph [8], in his monograph (p. 181), says: "Orr's assumption about the form of the disturbance which increases at the smallest Re is not correct since we shall see that the energy of an x-independent disturbance (streamwise perturbations) can increase when $\mathrm{Re} > \sqrt{1708}/2 \simeq 20.66$." (Here the values are rescaled in the interval $[-1, 1]$).

Joseph also gives a table of values of the principal eigenvalues (critical energy Reynolds numbers) which depend on a parameter τ, which varies from 0 (streamwise perturbations) to 1 (spanwise perturbations), and concludes that the value $\mathrm{Re} = 20.66$ is the limit for energy stability when $\tau = a = 0$ (streamwise perturbations), where a is the wave number in the x direction [8], p. 181.

However, *we prove here that the conclusion of Joseph [8] is not correct*. In fact, we note that Moffat [31] proved that the perturbations which are translationally invariant in the downstream direction are always nonlinearly energy stable. This means that $\mathrm{Re}^y = +\infty$, i.e., *the streamwise perturbations cannot destabilize the basic flows.*

Moreover, we prove that the critical Reynolds number for nonlinear stability of the basic motion with respect to "tilted perturbations" (perturbations with axes parallel to a tilted x' direction which form an angle θ with the x direction and which do not depend on x') are given by $\frac{\mathrm{Re}_{\mathrm{Orr}}}{\sin\theta} = \frac{44.3}{\sin\theta}$, $\theta \in (0, \frac{\pi}{2}]$, for any wave number.

This means that *the results of Orr are correct* both for linear (as we have shown in Sec. II) and nonlinear stability for 2D perturbations. We observe that local nonlinear stability results up to the Orr results are given by Kaiser *et al.* [25] and Kaiser and Mulone [26]. In those papers, the authors use the poloidal, toroidal, and mean flow representation of solenoidal vectors and define suitable weighted energies.

We observe that this result is also in agreement with what was observed by Reddy *et al.* [33] for the greatest transient linear growth: "For a given streamwise and spanwise wave number one can determine a disturbance, called an optimal,

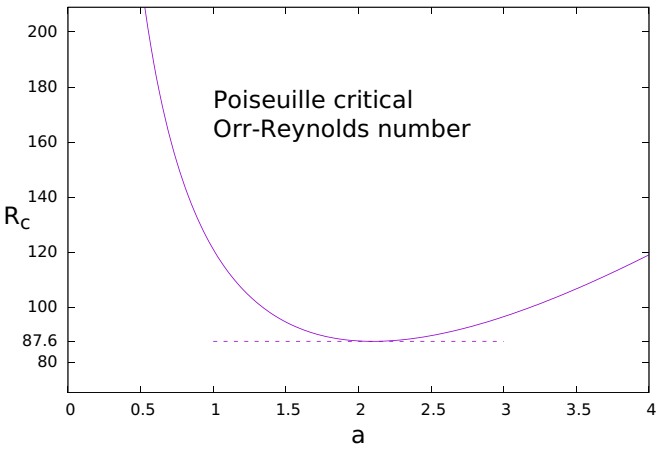

FIG. 2. Plane Poiseuille energy Orr-Reynolds number $\bar{R} = R_c$ as function of the wave number a, for Eq. (10) with nonslip boundary conditions. The absolute minimum is $R_c = 87.6$ and it is achieved when the wave number $a_c = 2.09$. Here the channel has gap 2 and $z \in [-1, 1]$.

which yields the greatest transient linear growth. In channel flows, the optimals which yield the most disturbance growth are independent, or nearly independent, of the streamwise coordinate" [33], p. 271.

From the result of Moffat [31], it can be proven that for streamwise perturbations, the time-decay coefficient of perturbations is $\pi^2/(2\mathrm{Re})$, and it is in agreement with the time-decay coefficient of streamwise perturbations of linearized equations.

In Fig. 1, we have plotted the critical energy Orr-Reynolds number, for plane Couette flow, as a function of the wave number a. The minimum critical Reynolds number obtained is 44.3. To solve the eigenvalue problem (10) with boundary conditions $w = w_z = 0$ at the boundaries $z = \pm 1$, we have used the Chebyshev-collocation method with 60 Chebyshev polynomials.

In Fig. 2, we have plotted the critical energy Orr-Reynolds number, for plane Poiseuille flow, as function of the wave number a. The minimum critical Reynolds number obtained is 87.6. To solve the eigenvalue problem (10) with boundary conditions $w = w_z = 0$ at the boundaries $z = \pm 1$, we have used the Chebyshev-collocation method with 60 Chebyshev polynomials.

Tilted perturbations

The experiments of Prigent *et al.* [15] show that at the onset of instability, some tilted perturbations appear (see Prigent *et al.* [15], Fig. 2). Here we consider tilted perturbations of an angle θ with the x direction, i.e., the perturbations $\mathbf{u}$, p along the x' axis which forms an angle $\theta \in (0, \frac{\pi}{2}]$ with the direction x and does not depend on x'. We prove that for "2.5-dimensional" (see Barkey and Tuckerman [16], p. 115) and 2D perturbations, the most destabilizing perturbations are the spanwise and the best stability results, in the energy norm, are those obtained by Orr [5]. Therefore, the results given by Joseph [21] and by Joseph and Carmi [22] *are not the best* because of a nonoptimal choice of an energy function.

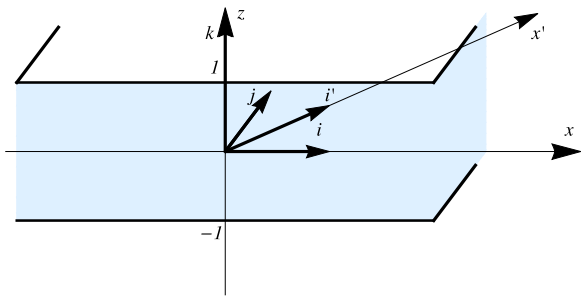

FIG. 3. Laminar flows in a horizontal channel. The direction of motion is that of the x axis. The direction of the x' axis forms an angle θ with the direction of the x axis.

For this, we consider an arbitrary inclined perturbation which forms an angle θ with the direction of motion $\mathbf{i}$ (the x direction, see Fig. 3).

We recall the well-known rotation transformation in the plane,

$$\begin{cases} x' = \cos\theta\, x + \sin\theta\, y \\ y' = -\sin\theta\, x + \cos\theta\, y, \end{cases} \qquad \begin{cases} \frac{\partial}{\partial x'} = \cos\theta\, \frac{\partial}{\partial x} + \sin\theta\, \frac{\partial}{\partial y} \\ \frac{\partial}{\partial y'} = -\sin\theta\, \frac{\partial}{\partial x} + \cos\theta\, \frac{\partial}{\partial y}. \end{cases} \tag{11}$$

The inverse transformations are easily obtained by substituting θ with $-\theta$ and exchanging x and x', y and y'.

Moreover,

$$\mathbf{u} = u\mathbf{i} + v\mathbf{j} + w\mathbf{k} = u'\mathbf{i}' + v'\mathbf{j}' + w\mathbf{k},$$

with

$$\begin{cases} u' = \cos\theta\, u + \sin\theta\, v \\ v' = -\sin\theta\, u + \cos\theta\, v, \end{cases} \tag{12}$$

and

$$\mathbf{i}' = \cos\theta\mathbf{i} + \sin\theta\mathbf{j}, \quad \mathbf{j}' = -\sin\theta\mathbf{i} + \cos\theta\mathbf{j}.$$

In the new variables, we have

$$\nabla' = \left(\cos\theta\, \frac{\partial}{\partial x'} - \sin\theta\, \frac{\partial}{\partial y'}\right)\mathbf{i} + \left(\sin\theta\, \frac{\partial}{\partial x'} + \cos\theta\, \frac{\partial}{\partial y'}\right)\mathbf{j} + \frac{\partial}{\partial z}\mathbf{k}, \quad \Delta' = \Delta.$$

Consider the perturbations system (4):

$$\begin{cases} u_t = -\mathbf{u}\cdot\nabla u + \mathrm{Re}^{-1}\Delta u - (f u_x + f' w) - \frac{\partial p}{\partial x} \\ v_t = -\mathbf{u}\cdot\nabla v + \mathrm{Re}^{-1}\Delta v - f v_x - \frac{\partial p}{\partial y} \\ w_t = -\mathbf{u}\cdot\nabla w + \mathrm{Re}^{-1}\Delta w - f w_x - \frac{\partial p}{\partial z} \\ \nabla\cdot\mathbf{u} = 0. \end{cases} \tag{13}$$

Multiply $(13)_1$ by $\cos\theta$, $(13)_2$ by $\sin\theta$, and add the equations so obtained. In addition, multiply $(13)_1$ by $-\sin\theta$, $(13)_2$ by $\cos\theta$, and add the equations so obtained.

Then, we have the system

$$\begin{cases} u'_t = -\mathbf{u}\cdot\nabla u' + \mathrm{Re}^{-1}\Delta u' - (f u'_x + f'\cos\theta\, w) - \frac{\partial p}{\partial x'} \\ v'_t = -\mathbf{u}\cdot\nabla v' + \mathrm{Re}^{-1}\Delta v' - f v'_x + f'\sin\theta\, w - \frac{\partial p}{\partial y'} \\ w_t = -\mathbf{u}\cdot\nabla w + \mathrm{Re}^{-1}\Delta w - f w_x - \frac{\partial p}{\partial z} \\ \frac{\partial u'}{\partial x'} + \frac{\partial v'}{\partial y'} + \frac{\partial w}{\partial z} = 0. \end{cases} \tag{14}$$

We note that if $\theta \to 0$, then $x' \to x$, $y' \to y$, $u' \to u$, $v' \to v$.

Now we consider *tilted (stream) perturbations in the x' direction*, i.e., those with $\frac{\partial}{\partial x'} \equiv 0$. The first equation of (14) becomes

$$u'_t = -\mathbf{u}\cdot\nabla u' + \mathrm{Re}^{-1}\Delta u' - (f u'_x + f'\cos\theta\, w). \tag{15}$$

We have the energy equation

$$\frac{d}{dt}\left[\frac{\beta\|u'\|^2}{2}\right] = -\beta(f'\cos\theta u', w) - \beta\mathrm{Re}^{-1}\|\nabla u'\|^2, \tag{16}$$

where β is an arbitrary positive number to be chosen. (In the Appendix, Sec. 1, we prove the decay of u' to zero if $\mathrm{Re} < \bar{R}$).

Moreover, we have

$$\frac{d}{dt}\left[\frac{\|v'\|^2 + \|w\|^2}{2}\right] = -\mathrm{Re}^{-1}(\|\nabla v'\|^2 + \|\nabla w)\|^2 + (f'\sin\theta\, v', w). \tag{17}$$

We note that as $\theta \to 0$, the energy equations tend to the energy equations obtained for the streamwise perturbations. Moreover, in the case $\frac{\partial}{\partial x'} \equiv 0$, if $\theta \to \frac{\pi}{2}$, since $y' \to -x$, $v' \to -u$, $x' \to y$, $\frac{\partial v'}{\partial y'} \to \frac{\partial u}{\partial x}$, the energy equation (17) becomes that for spanwise perturbations.

Defining

$$H = \tfrac{1}{2}[\|v'\|^2 + \|w\|^2], \tag{18}$$

we have

$$\begin{aligned} \dot{H} &= (f'\sin\theta\, v', w) - \mathrm{Re}^{-1}[\|\nabla v'\|^2 + \|\nabla w\|^2] \\ &\leqslant \left(\frac{1}{\bar{R}} - \frac{1}{\mathrm{Re}}\right)[\|\nabla v'\|^2 + \|\nabla w\|^2], \end{aligned} \tag{19}$$

where

$$\frac{1}{\bar{R}} = \max_{\mathcal{S}} \frac{(f'\sin\theta\, v', w)}{\|\nabla v'\|^2 + \|\nabla w\|^2}, \tag{20}$$

and $\mathcal{S}$ is the space of the *kinematically admissible fields*,

$$\begin{aligned} \mathcal{S} = \{&v', w \in H^1(\Omega),\ \ v' = w = 0 \quad \text{on the boundaries}, \\ &v'_{y'} + w_z = 0, \quad \|\nabla v'\| + \|\nabla w\| > 0\}. \end{aligned} \tag{21}$$

It is not hard to prove (see the Appendix, Sec. 2) that for a fixed wavelength λ,

$$\bar{R} = \mathrm{Re}_{\mathrm{Orr}}\left(\frac{2\pi}{\lambda\sin\theta}\right)\Big/\sin\theta. \tag{22}$$

In particular, we note that for $\theta \to \frac{\pi}{2}$, we obtain the critical Orr-Reynolds number for spanwise perturbations. For $\theta \to 0$, we obtain that the critical Reynolds number tends to $+\infty$ (in agreement with the result of Moffat [31]).

From (22), we see that the $\bar{R}$ does not change if we substitute θ with $-\theta$. Thus we may exchange the variables, i.e., we may consider a domain aligned with the pattern wave vector and thus tilted relative to the streamwise-spanwise directions of the flow and obtain the same critical Reynolds number.

Formula (22) gives the critical value for a fixed positive wavelength λ. The minimum with respect to λ in $(0, +\infty)$ is the nonlinear critical Reynolds number for tilted perturbations of an angle θ:

$$\bar{R}_c = \min_{\lambda>0} \mathrm{Re}_{\mathrm{Orr}}\left(\frac{2\pi}{\lambda\sin\theta}\right)\Big/\sin\theta = \mathrm{Re}_{\mathrm{cOrr}}/\sin\theta, \tag{23}$$

where $\mathrm{Re}_{\mathrm{cOrr}} = 44.3$ for plane Couette flow and $\mathrm{Re}_{\mathrm{cOrr}} = 87.6$ for plane Poiseuille flow.

The meaning of (23) is that when the Reynolds number is less than $\bar{R}_c$, the linear and nonlinear energy of tilted perturbations of an angle θ and arbitrary wavelength λ decay exponentially fast as $t \to +\infty$. For instance, if we consider tilted perturbations of an angle $\theta = 25^\circ$, the critical energy Reynolds number is $\bar{R}_c = 104.82$ for plane Couette flow and $\bar{R}_c = 207.51$ for plane Poiseuille flow, for any λ. These values, though lower than the experimental or numerical values, however, are bigger than the classical ones.

In the next section, we compare our critical Reynolds energy stability results for a given inclination angle and a *fixed wavelength* with the values obtained in the experiments and numerical simulations.

IV. COMPARISON WITH EXPERIMENTAL AND NUMERICAL RESULTS AND FINAL COMMENTS

In order to compare the critical Reynolds numbers with the experiments and the numerical simulations, we must return to (22) with fixed wavelengths. It is clear that if we choose a particular wavelength, the values $\bar{R}_c = 104.82$ for plane Couette flow and $\bar{R}_c = 207.51$ for plane Poiseuille flow, in general, will increase in value.

For instance, if we consider the case of the experiments of Prigent *et al.* [15] (see also Fig. 29 of Barckley and Tuckerman [16]), we have

(i) $\theta = 25^\circ$, $\lambda = 46$, experimental Reynolds number is about 395, and here we obtain approximately $\bar{R} = 369$;

(ii) $\theta = 26^\circ$, $\lambda = 48$, experimental Reynolds number is about 385, and here we obtain approximately $\bar{R} = 383$;

(iii) $\theta = 27,5^\circ$, $\lambda = 51$, experimental Reynolds number is about 375, and here we obtain approximately $\bar{R} = 404$;

(iv) (simulation of Barckley and Tuckerman [16]) $\theta = 24^\circ$, $\lambda = 40$, Reynolds number is about 350, and here we obtain approximately $\bar{R} = 325$; and

(v) $\theta = 30^\circ$, $\lambda = 57$, experimental Reynolds number is about 350, and here we obtain approximately $\bar{R} = 450$ and $R = 398$ in [16].

In Fig. 4, we have plotted a continuous curve which is a part of the prolongation of the curve given in Fig. 1 where the abscissa of its points is in the interval (0.2,0.4), and we have signed the five critical values reported in Sec. IV from (i) to (v). The points on the curve correspond to our critical Reynolds numbers; the other points with the same symbols and colors are those obtained in the experiments and numerical simulations.

In the case of *Poiseuille flow*, the result of Tsukahara *et al.* [17] is converted to a uniform Reynolds number based on

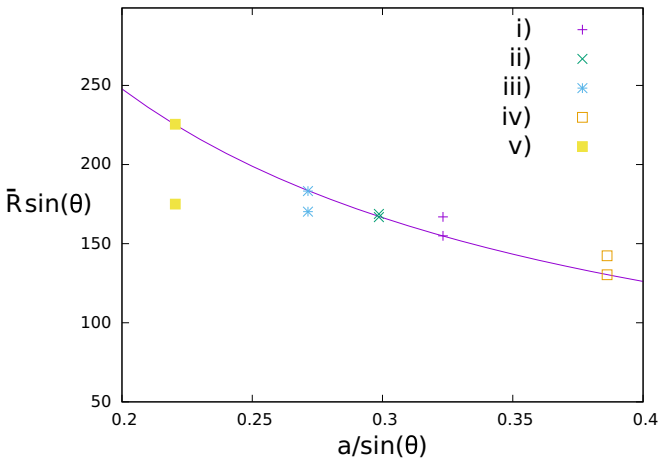

FIG. 4. Couette energy Orr-Reynolds numbers given by formula (25): we plot the five critical values reported in Sec. IV from (i) to (v), as indicated here by the different points. We have also added the continuous curve that for fixed ratio $\frac{a}{\sin\theta} = \frac{2\pi}{\lambda \sin\theta}$, gives $\mathrm{Re}_{\mathrm{Orr}}(\frac{2\pi}{\lambda \sin\theta})$. On the curve, we have reported our corresponding critical Reynolds values.

the average shear and half gap [see Barckley and Tuckerman [16], Table 3, and (A12)]. Now the nondimensional channel is $\mathcal{D}_{2P} = \mathbb{R}^2 \times [-2, 2]$ and

$$\mathbf{U} = f(z)\mathbf{i} = \left(1 - \frac{z^2}{4}\right)\mathbf{i}. \tag{24}$$

The Orr equation we get is

$$-\frac{\bar{R}\sin\theta}{4}(w_x + 2zw_{xz}) + \Delta\Delta w = 0,$$

where now we need to replace x with $x\sin\theta$, with boundary conditions $w = w_z = 0$ on the boundaries $z = \pm 2$.

By making the substitution $Z = 2z$ (22), and also rescaling the variable x, it is easy to verify that we obtain the same values for $\bar{R}$ in (22) but now divided by 2:

$$\bar{R} = \mathrm{Re}_{\mathrm{Orr}}\left(\frac{2\pi}{\lambda \sin\theta}\right) \Big/ (2\sin\theta), \tag{25}$$

where now $\mathrm{Re}_{\mathrm{Orr}}(\frac{2\pi}{\lambda \sin\theta})$ is the Orr number for Poiseuille flow evaluated at $\frac{2\pi}{\lambda \sin\theta}$.

In particular, if we consider the values in [17], we have $\theta = 24^\circ$, $\lambda = 41$. The Reynolds number obtained in [17] [see [16] (A12)] is about 357; here we obtain approximately $\bar{R} = 355$.

From these results, both in the Couette and Poiseuille cases, we see that the critical energy Reynolds numbers that we find are in a very good agreement with the experiments and the simulations. However, when the inclination angle increases (such as in the cases $\theta = 30^\circ$ to $\theta = 37^\circ$), our critical values increase, as for the results of Barckley and Tuckerman [16], while the critical values obtained in the experiments by Prigent *et al.* [15] decrease. This is not clear. What we can say is that for Reynolds numbers less than $\bar{R}$, the energy of tilted perturbations (streamwise rolls) must decay. These rolls probably appear at the onset of instability, as observed by Prigent *et al.* [34]. In fact, in the final part of their paper, Prigent *et al.* [34] summarize their results: "we have presented...(i) turbulent spirals and spots are essentially the same in PCF...(ii) all our observations are fully captured by the dynamics of coupled amplitude equations with noise. Taken together, these results suggest the possibility of a large-wavelength instability within fully turbulent shear flows. The precise origin of such an instability is at present completely unknown. The work by Hegseth [35] suggests it is related to the emergence of vortex type structures in the streamwise direction" [34], p. 014501–4.

Barkley and Tuckerman [16] studied numerically a turbulent-laminar banded pattern in plane Couette flow which is oriented obliquely to the streamwise direction. In particular, in [16], the authors present a detailed analysis of the new turbulent-laminar patterns in large aspect-ratio shear flows discovered in recent years by researchers at GIT-Saclay [15] (see Fig. 1 in [16]). They observe that "the patterns are always found near the minimum Reynolds numbers for which turbulence can exist in the flow" [16], p. 111.

The critical energy Reynolds numbers we obtain are in a good agreement with the experiments and the numerical simulations. Since experimentally the patterns are found near the *minimum* Reynolds numbers, the energy Reynolds numbers capture the physics of the problem well. As we have remarked, the energy method gives sufficient stability (both linear and nonlinear) conditions of the basic flows against tilted perturbations. The critical Reynolds numbers are obtained from the energy equation (the Orr-Reynolds method) (17) with some estimates from above (19); therefore, we obtain only sufficient stability conditions. If one will be able to prove that $\dot{H}$ is positive for some Reynolds number, this will give instability results, but it is very difficult to prove that with the energy method.

We also remark that since the cubic terms $(-\mathbf{u}\cdot\nabla u', u')$, $(-\mathbf{u}\cdot\nabla v', v')$, $(-\mathbf{u}\cdot\nabla w, w)$ vanish, the critical energy Reynolds numbers are the same for linear and nonlinear perturbation systems. Obviously, the nonlinear terms are responsible for the turbulence and chaos that appear for high Reynolds numbers.

Now we make a comparison of our Reynolds numbers with those obtained by [16]. They found a "good first approximation for the relationship between Re, λ and θ: $\mathrm{Re}\sin\theta \approx \pi\lambda$" [cf. [16] (4.2), p. 133]. They also said: "Equation (4.2) captures the correct order of magnitude of $\mathrm{Re}\sin\theta/\lambda$; specifically $1.8 \lesssim \mathrm{Re}\sin\theta/\lambda \lesssim 5$. Moreover, in figure 29 one sees that for fixed Re, λ increases with increasing θ, as (4.2) predicts. Equation (4.2) does not hold in detail, however. Most notably, figure 29 shows that when Re is decreased at fixed θ, the wavelength λ increases rather than decreases as one would expect from (4.2)" [16], p. 133.

In Fig. 5, we have compared our energy Orr-Reynolds numbers $\bar{R} = R_c$ as a function of the wavelength λ and the values obtained by [16], $\mathrm{Re} = \frac{\pi\lambda}{\sin 24^\circ}$, for $\theta = 24^\circ$. We obtain a *very good agreement* of these values. If we had used $R_c = \frac{3.56\lambda}{\sin 24^\circ}$ in the simulation of [16], then the dashed line would have been above the continuous line in Fig. 5 because all the values would have increased by a factor of $3.56/\pi$.

We also note that our Reynolds numbers, for the fixed inclination angle, increase with λ as in [16].

Finally:

(i) We underline that the results we have obtained here continue to hold for arbitrary plane parallel shear flows. For this, it is sufficient to compute the maximum m given by (A4).

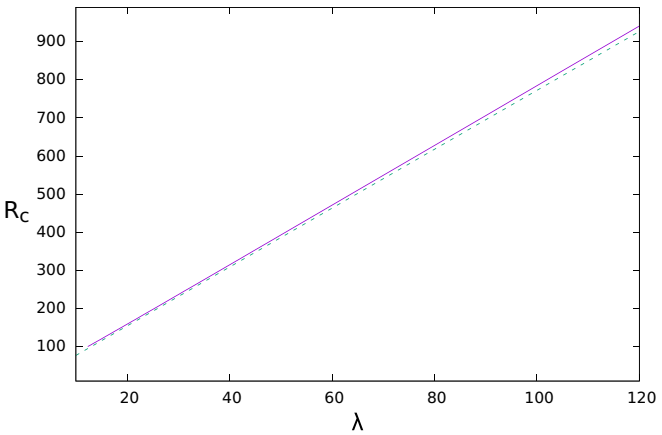

FIG. 5. Comparison of our energy Orr-Reynolds numbers $\bar{R} = R_c$ as a function of the wavelength λ and the values obtained by [16], formula (4.2), $\mathrm{Re} = \frac{\pi\lambda}{\sin 24^\circ}$. The dashed line represents $R_c = \frac{\pi\lambda}{\sin 24^\circ}$; the continuous line represents our critical Reynolds values $\bar{R} = R_c$ as a function of λ.

(ii) We remark that the energy method (applied both in the linear and nonlinear case) provides thresholds of stability and it is not able to capture the details of the fully developed turbulent regime. However, our work reveals a connection between wave numbers and critical Reynolds numbers in these two very different regimes.

(iii) The method used here can also be applied to magnetohydrodynamics plane Couette and Hartmann shear flows. This will be done in a future paper.

(iv) We believe that the results obtained in the present paper make a contribution to the solution of the Couette-Sommerfeld paradox.

ACKNOWLEDGMENTS

We thank Prof. Eckhardt for notifying us of the work of Moffat and for his helpful comments. We also thank two anonymous referees for their comments and observations which have led to improvements in the paper.

The research that led to the present paper was partially supported by the group GNFM of Istituto Nazionale di Alta Matematica "Francesco Severi", by the University of Catania, Grant No. PTRDMI-53722122113. The authors also acknowledge support from: Project No. PON SCN 00451 CLARA - CLoud plAtform and smart underground imaging for natural Risk Assessment, Smart Cities and Communities and Social Innovation; Grant 2017YBKNCE of national project PRIN of Italian Ministry for University and Research.

APPENDIX

1. Decay of u'

It is easy to prove that the component u' in (16) also tends to zero as $t \to \infty$ if $\mathrm{Re} < \bar{R}$. In fact, by defining

$$E(t) = \frac{1}{2}[\|v'\|^2 + \|w\|^2] + \frac{\beta\|u'\|^2}{2}, \quad \beta > 0, \tag{A1}$$

the constant β is a positive number that we can properly choose.

The (Orr-Reynolds) energy equation is

$$\dot{E} = -\beta\mathrm{Re}^{-1}\|\nabla u'\|^2 - \beta(f'\cos\theta\, u', w) - \mathrm{Re}^{-1}(\|\nabla v'\|^2 + \|\nabla w\|^2) + (f'\sin\theta\, v', w). \tag{A2}$$

Now define

$$r = \frac{1}{\bar{R}} - \frac{1}{\mathrm{Re}}$$

and suppose $r < 0$, i.e., $\mathrm{Re} < \bar{R}$. Since, for functions f of the Sobolev space $H^1(\Omega)$ which vanish at the boundaries $z = \pm 1$, the Poincaré inequality $\pi^2\|f\|^2 \leqslant \|\nabla f\|^2$ holds, we have the following estimate:

$$\dot{E} \leqslant -r\pi^2(\|v'\|^2 + \|w\|^2) + m\beta\|w\|\|u'\| - \beta\mathrm{Re}^{-1}\pi^2\|u'\|^2, \tag{A3}$$

where

$$m = \max_{[-1/2,1/2]} |f'(z)|\cos\theta. \tag{A4}$$

We first note that if $\theta = \frac{\pi}{2}$, then the right-hand side of the previous inequality is always negative for $r > 0$. We consider the case of $\theta < \frac{\pi}{2}$.

By arithmetic-geometric mean inequality, we have

$$m\beta\|u'\|\|w\| \leqslant \frac{\beta m^2}{2\epsilon}\|w\|^2 + \frac{\beta\epsilon}{2}\|u'\|^2, \tag{A5}$$

where ϵ is an arbitrary positive number to be chosen.

Therefore,

$$\dot{E} \leqslant \left(\frac{\beta m^2}{2\epsilon} - r\pi^2\right)\|w\|^2 - r\pi^2\|v'\|^2 + \beta\left(\frac{\epsilon}{2} - \mathrm{Re}^{-1}\pi^2\right)\|u'\|^2. \tag{A6}$$

By choosing $\epsilon = \frac{\pi^2}{\mathrm{Re}}$ and $\beta = \frac{r\pi^4}{m^2\mathrm{Re}}$, we obtain

$$\dot{E} \leqslant -\frac{r\pi^2}{2}(\|w\|^2 + \|v'\|^2 + \beta\|u'\|^2) = -r\pi^2 E. \tag{A7}$$

Taking into account that $\mathrm{Re} < \bar{R}$, i.e., $r > 0$, we finally have

$$E(t) \leqslant E(0)e^{-r\pi^2 t}. \tag{A8}$$

This means that the energy $E(t)$ goes exponentially to zero. In particular, all the components $\|v'\|, \|w\|, \|u'\|$ of the energy go to zero as $t \to +\infty$.

2. Critical energy Reynolds number (22)

The Euler-Lagrange equations of the maximum problem (20) are

$$\bar{R}\sin\theta(f'w\mathbf{j}' + f'v'\mathbf{k}) + 2(\Delta v'\mathbf{j}' + \Delta w\mathbf{k}) = \nabla\mu, \tag{A9}$$

where μ is a Lagrange multiplier. By taking the third component of the *double curl* of this equation, we have

$$\frac{\bar{R}\sin\theta}{2}(f''w_{y'} + f'w_{y'z} - f'v'_{y'y'}) - \Delta\Delta w = 0. \tag{A10}$$

Since, by solenoidality condition, $\frac{\partial v'}{\partial y'} = -\frac{\partial w}{\partial z}$, and $\Delta = \Delta'$, we obtain

$$\frac{\bar{R}\sin\theta}{2}(f''w_{y'} + 2f'w_{y'z}) - \Delta'\Delta' w = 0. \tag{A11}$$

By defining $\tilde{y} = -y'$, the operator Δ' does not change and we have

$$\frac{\bar{R}\sin\theta}{2}(f''w_{\tilde{y}} + 2f'w_{\tilde{y}z}) + (w_{\tilde{y}\tilde{y}\tilde{y}\tilde{y}} + 2w_{\tilde{y}\tilde{y}zz} + w_{zzzz}) = 0. \tag{A12}$$

Since we are considering streamwise perturbations in the direction x', we have $\frac{\partial}{\partial x'} = 0$. From $\frac{\partial}{\partial x} = \frac{\partial}{\partial x'}\cos\theta - \frac{\partial}{\partial y'}\sin\theta$, we have $\frac{\partial}{\partial x} = -\frac{\partial}{\partial y'}\sin\theta = \frac{\partial}{\partial \tilde{y}}\sin\theta$. Therefore, the last equation becomes

$$\frac{\bar{R}\sin\theta}{2}\left(f''\frac{w_x}{\sin\theta} + 2f'\frac{w_{xz}}{\sin\theta}\right) + \left(\frac{w_{xxxx}}{\sin^4\theta} + 2\frac{w_{xx}}{\sin^2\theta} + w_{zzzz}\right) = 0. \tag{A13}$$

This equation is linear and has coefficients which do not depend on x. We may look for solutions of the kind $w(x,z) = e^{iax}W(z)$ to obtain

$$\frac{\bar{R}\sin\theta}{2}\left(f''\frac{ia}{\sin\theta}W + 2f'\frac{ia}{\sin\theta}W'\right) + \left(\frac{a^4}{\sin^4\theta}W - 2\frac{a^2}{\sin^2\theta}W'' + W^{iv}\right) = 0. \tag{A14}$$

This equation coincides with the celebrated Orr equation if we substitute the critical Reynolds number $\mathrm{Re}_{\mathrm{Orr}}$ in that equation with $\bar{R}\sin\theta$ and evaluate $\mathrm{Re}_{\mathrm{Orr}}$ at the wave number a divided by $\sin\theta$, $\frac{a}{\sin\theta} = \frac{2\pi}{\lambda\sin\theta}$. a is the wave number in the direction orthogonal to the streamwise direction x' and λ is its wavelength; therefore,

$$\bar{R} = \mathrm{Re}_{\mathrm{Orr}}\left(\frac{2\pi}{\lambda\sin\theta}\right)\Big/\sin\theta. \tag{A15}$$

[1] M. M. Couette, Études sur le frottement des liquides, Ann. Chim. Phys. **21**, 433 (1890).

[2] J. L. M. Poiseuille, Experimental studies on the movement of liquids in tubes of very small diameters, Ann. Phys. **134**, 424 (1843).

[3] L. Kelvin, Stability of fluid motion-rectilinear motion of viscous fluid between two parallel plates, Philos. Mag. **24**, 188 (1887).

[4] O. Reynolds, An experimental investigation of the circumstances which determine whether the motion of water shall be direct or sinuous, and of the law of resistance in parallel channels, Proc. R. Soc. London **35**, 84 (1883).

[5] W. M'F. Orr, The stability or instability of the steady motions of a perfect liquid and of a viscous liquid, Proc. Roy. Irish Acad. Sect. A: Mathe. Phys. Sci. **27**, 69 (1907).

[6] A. Sommerfeld, A contribution to the hydrodynamic explanation of the turbulent fluid movements, in *Proceedings of the 4th International Congress of Mathematicians, Rome* (Accademia dei Lincei, Roma, 1908), Vol. III, p. 116.

[7] H. B. Squire, On the stability of three-dimensional disturbances of viscous flow between parallel walls, Proc. R. Soc. A **142**, 621 (1933).

[8] D. D. Joseph, *Stability of Fluid Motions I* (Springer-Verlag, Berlin, 1976).

[9] F. H. Busse, A Property of the energy stability limit for plane parallel shear flow, Arch. Rat. Mech. Anal. **47**, 28 (1972).

[10] Y. Deng and N. Masmoudi, Long time instability of the Couette flow in low Gevrey spaces, arXiv:1803.01246.

[11] J. Bedrossian, P. Germain and N. Masmoudi, On the stability threshold for 3D Couette flow in Sobolev regularity, Ann. Math. **185**, 541 (2017).

[12] Y. Lan and Y. C. Li, A resolution of the turbulence paradox: Numerical implementation, Int. J. Non-Linear Mech. **51**, 1 (2013).

[13] S. Cherubini and P. De Palma, Nonlinear optimal perturbations in a Couette flow: Bursting and transition, J. Fluid Mech. **716**, 251 (2013).

[14] M. Liefvendahl and G. Kreiss, Bounds for the threshold amplitude for plane Couette flow, J. Nonlinear Math. Phys. **9**, 311 (2002).

[15] A. Prigent, G. Grégoire, H. Chaté, and O. Dauchot, Long-wavelength modulation of turbulent shear flows, Physica D **174**, 100 (2003).

[16] D. Barkley and L. S. Tuckerman, Mean flow of turbulent-laminar patterns in plane Couette flow, J. Fluid Mech. **576**, 109 (2007).

[17] T. Tsukahara, Y. Seki, H. Kawamura, and D. Tochio, DNS of turbulent channel flow at very low Reynolds numbers, in *Proceedings of the 4th International Symposium on Turbulence and Shear Flow Phenomena, Williamsburg, VA, USA, 2005* (2005), pp. 935–940, arXiv:1406.0248.

[18] S. A. Orszag, Accurate solution of the Orr-Sommerfeld stability equation, J. Fluid Mech. **50**, 689 (1971).

[19] V. Romanov, Stability of plane-parallel Couette flow, Funct. Anal. Appl. **7**, 137 (1973).

[20] O. Zikanov, On the instability of pipe Poiseuille flow, Phys. Fluids **8**, 2923 (1996).

[21] D. D. Joseph, Eigenvalue bounds for the Orr-Sommerfeld equation, J. Fluid Mech. **33**, 617 (1966).

[22] D. D. Joseph and S. Carmi, Stability of Poiseuille flow in pipes, annuli and channels, Quart. App. Math. **26**, 575 (1969).

[23] B. Straughan, *The Energy Method, Stability and Nonlinear Convection*, Applied Mathematical Sciences 91, 2nd ed. (Springer-Verlag, New York, 2004).

[24] S. Rionero and G. Mulone, On the non-linear stability of parallel shear flows, Continuum Mech. Thermodyn. **3**, 1 (1991).

[25] R. Kaiser, A. Tilgner, and W. vonWahl, A generalized energy functional for plane Couette flow, SIAM J. Math. Anal. **37**, 438 (2005).

[26] R. Kaiser and G. Mulone, A note on nonlinear stability of plane parallel shear flows, J. Math. Anal. Appl. **302**, 543 (2005).

[27] Y. Li, Z. Lin, A resolution of the Sommerfeld paradox, SIAM J. Math. Anal. **43**, 1923 (2011).

[28] K. M. Butler and B. F. Farrell, Three-dimensional optimal perturbations in viscous shear flow, Phys. Fluids A **4**, 1637 (1992).

[29] D. Barkley and L. S. Tuckerman, Stability analysis of perturbed plane Couette flow, Phys. Fluids **11**, 1187 (1999).

[30] D. Barkley and L. S. Tuckerman, Computational Study of Turbulent Laminar Patterns in Couette Flow, Phys. Rev. Lett. **94**, 014502 (2005).

[31] K. Moffatt, Fixed points of turbulent dynamical systems and suppression of nonlinearity, in *Whither Turbulence*, edited by J. Lumley (Springer, Berlin Heidelberg, 1990), p. 250.

[32] P. G. Drazin and W. H. Reid, *Hydrodynamic Stability*, Cambridge Monographs on Mechanics, 2nd ed. (Cambridge University Press, Cambridge, 2004).

[33] S. C. Reddy, P. J. Schmid, J. S. Baggett and D. S. Henningson, On stability of streamwise streaks and transition thresholds in plane channel flows, J. Fluid Mech. **365**, 269 (1998).

[34] A. Prigent, G. Grégoire, H. Chaté, O. Dauchot, and W. van Saarloos, Large-Scale Finite-Wavelength Modulation within Turbulent Shear Flows, Phys Rev. Lett. **89**, 014501 (2002)

[35] J. J. Hegseth, Turbulent spots in plane Couette flow, Phys. Rev. E **54**, 4915 (1996).